Novel Synthesis and Photocatalytic Activity of Oxysulfide Sm$_2$Ti$_2$S$_2$O$_5$

Akio Ishikawa,[†] Yoko Yamada,[†] Tsuyoshi Takata,[†] Junko N. Kondo,[†] Michikazu Hara,[†] Hisayoshi Kobayashi,[‡] and Kazunari Domen*[,†,§]

Chemical Resources Laboratory, Tokyo Institute of Technology, Nagatsuta 4259, Midori-ku, Yokohama 226-8503, Japan, Department of Chemistry and Bioscience, Kurashiki University of Science and the Arts, Nishinoura 2640, Tsurajima, Kurashiki, 712-8505, Japan, Core Research for Evolutional Science and Technology, Japan Science and Technology Corp. (CREST, JST), 2-1-13 Higashiueno, Taito-ku, Tokyo 110-0015, Japan

The oxysulfide Sm$_2$Ti$_2$S$_2$O$_5$ was synthesized by sulfurization of Sm$_2$Ti$_2$O$_7$ under H$_2$S flow. Amorphous Sm$_2$Ti$_2$O$_7$ was found to be the most appropriate precursor for the synthesis of Sm$_2$Ti$_2$S$_2$O$_5$ at temperatures above 1073 K. The relationship between the preparation conditions and the photocatalytic activities for H$^+$ reduction to H$_2$ and H$_2$O oxidation to O$_2$ was investigated, and the highest activities for both H$_2$ and O$_2$ evolution were obtained at a sulfurization temperature of 1123 K. Subsequent heating of Sm$_2$Ti$_2$S$_2$O$_5$ in air enhanced the activities further. Sulfurization by H$_2$S allows for synthesis of Sm$_2$Ti$_2$S$_2$O$_5$ at lower temperatures with a significantly shorter heating period (1 h) than that of conventional solid-state reaction.

Introduction

Oxysulfides have recently attracted considerable attention due to the interesting physical properties these materials exhibit, including superconductivity[1] and charge density wave character.[2] We have been interested in utilizing various oxides and other materials as photocatalysts for overall water splitting to accomplish conversion of photon energy into chemical energy,[3–5] and have already reported on the utility of the oxysulfide Sm$_2$Ti$_2$S$_2$O$_5$ as a stable photocatalyst.[6] Under visible light (440 nm $\leq \lambda \leq$ 650 nm) irradiation, Sm$_2$Ti$_2$S$_2$O$_5$ with a band gap of ca. 2 eV evolves H$_2$ or O$_2$ from aqueous solutions containing a sacrificial electron donor (Na$_2$S–Na$_2$SO$_3$ or methanol) or acceptor (Ag$^+$) without noticeable degradation. In previous work, Sm$_2$Ti$_2$S$_2$O$_5$ was obtained by calcining a mixture of Sm$_2$S$_3$, Sm$_2$O$_3$, and TiO$_2$ powders at 1273 K in an evacuated sealed quartz tube,[6] according to a previously reported solid-state reaction method.[1] This solid-state method requires calcination for 2 weeks at 1273 K because of the slow reaction rate at the solid–solid boundary. However, the Sm$_2$Ti$_2$S$_2$O$_5$ material prepared at such high temperature

over a long period has large particle size, which is undesirable for use as a catalyst. Physically, smaller particles result in a shortened diffusion length for photogenerated electron–hole pairs, leading to less recombination of electron–hole pairs and enhanced photocatalytic activity. Therefore, the use of fine particles with good crystallinity is favorable for photocatalysis. As it is difficult to synthesize fine particles of Sm$_2$Ti$_2$S$_2$O$_5$ by the solid-state method, we developed a new synthetic route to Sm$_2$Ti$_2$S$_2$O$_5$ using H$_2$S. The method is presented here, along with a comparison of the photocatalytic activity of the new material with that of the material prepared by the solid-state method.

Experimental Section

Synthesis of Sm$_2$Ti$_2$S$_2$O$_5$. Samarium titanate Sm$_2$Ti$_2$O$_7$ was prepared by the polymerized complex method[7] using Ti(OiPr)$_4$ and Sm(NO$_3$)$_3$·6H$_2$O as starting materials. Ethylene glycol and methanol were employed as solvents, and anhydrous citric acid was employed as a complexing agent to immobilize Ti and Sm ions. After polymerization of a mixture containing stoichiometric amounts of Sm and Ti (Sm/Ti = 1:1) according to the method in the literature,[8] samarium titanates were obtained by calcination at various temperatures in air. This samarium titanate Sm$_2$Ti$_2$O$_7$ is referred to as the oxide precursor. Sm$_2$Ti$_2$S$_2$O$_5$ was prepared from the oxide precursor (0.5 g) by calcination under flowing H$_2$S (flow rate 10 mL·min^{-1}) at various temperatures. This synthesis method is abbreviated as the HGS (H$_2$S gas sulfurization) method, and the solid-state reaction of Boyer-Candalen et al.[1] is abbreviated as the SSR (solid-state reaction) method.

Characterization of Catalysts. The prepared samples were characterized by X-ray powder diffraction (XRD; Geiger-

---

(1) Boyer-Candalen, C.; Meerschaut, A. *Chemistry* **1999**, *2*, 93.

(2) Goga, M.; Seshadri, R.; Ksenofontov, V.; Gütlich, P.; Tremel, W. *Chem. Commun.* **1999**, 979.

(3) Domen, K.; Kudo, A.; Ohnishi, T. *J. Catal.* **1986**, *102*, 92.

(4) Takata, T.; Furumi, Y.; Shinohara, K.; Tanaka, A.; Hara, M.; Kondo, J. N.; Domen, K. *Chem. Mater.* **1997**, *9*, 1063.

(5) Kudo, A.; Tanaka, K.; Domen, K.; Maruya, K.; Aika, K.; Onishi, T. *J. Catal.* **1988**, *111*, 67.

(6) Ishikawa, A.; Takata, T.; Kondo, J. N.; Hara, M.; Kobayashi, H.; Domen, K. *J. Am. Chem. Soc.* **2002**, *124*, 13547.

(7) Kakihana, M. *J. Sol-Gel Sci.* **1996**, *5*, 7.

(8) Hitoki, G.; Ishikawa, A.; Takata, T.; Kondo, J. N.; Hara, M.; Domen, K. *Chem. Lett.* **2002**, 736.
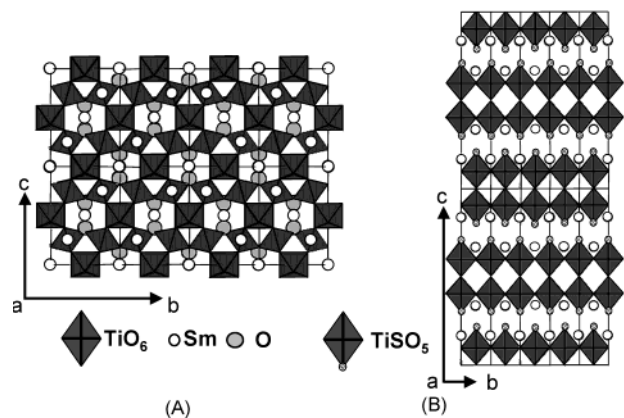
**Figure 1.** Schematic structures of (A) Sm$_2$Ti$_2$O$_7$ and (B) Sm$_2$Ti$_2$S$_2$O$_5$.

flex RAD-B, Rigaku; Cu Kα), field-emission scanning electron microscopy (FE-SEM; S-4700, Hitachi), field-emission transmission electron microscopy (FE-TEM; JEM-2010F, JEOL), ultraviolet−visible diffuse reflectance spectroscopy (UV−vis DRS; V-560, Jasco), and X-ray photoelectron spectroscopy (XPS; ESCA 3200, Shimadzu).

Photocatalytic Reactions. Photocatalytic reactions were carried out in a closed gas circulation system under irradiation with visible light ($\lambda \geq 440$ nm) from a Xe lamp (300 W) via a cutoff filter. The catalyst (0.2 g) was suspended in an aqueous solution (200 mL) under magnetic stirring. A sacrificial electron donor (0.01 M Na$_2$S−0.01 M Na$_2$SO$_3$) or sacrificial electron acceptor (0.01 M AgNO$_3$) was employed for H$_2$ or O$_2$ evolution, respectively. For H$_2$ evolution, Pt was loaded by impregnation from H$_2$PtCl$_6$ followed by reduction in H$_2$ at 473 K. The apparent quantum efficiencies (Φ) were calculated using the equation: QE (%) = (AR/I) × 100, where A, R, and I are coefficients based on the reactions (H$_2$ evolution, 2; O$_2$ evolution, 4), the H$_2$ or O$_2$ evolution rate (molecules h^{-1}), and the rate of absorption of incident photons (8.6×10^{21} photons h^{-1} at 440 nm $\leq \lambda \leq$ 650 nm based on the total photon number reaching the reaction vessel).

Results and Discussion

Preparation of Oxide Precursor for Sulfurization. Figure 1 shows the schematic structures of Sm$_2$Ti$_2$O$_7$ and Sm$_2$Ti$_2$S$_2$O$_5$. The crystal system of Sm$_2$Ti$_2$S$_2$O$_5$ is tetragonal with space group $I4/mmm$, whereas Sm$_2$Ti$_2$O$_7$ has cubic symmetry with space group $Fd\bar{3}m$. The effect of calcination temperature of the oxide precursor was investigated to produce a sample appropriate for sulfurization. The polymers obtained by the polymerized complex method were calcined in air, and oxide precursors were obtained at temperatures above 773 K. Figure 2 shows the XRD patterns of the oxide precursors prepared by calcination at various temperatures between 773 and 1473 K. Crystallization occurred for Sm$_2$Ti$_2$O$_7$ at 1073 K and above, and the intensities of the diffraction peaks produced by Sm$_2$Ti$_2$O$_7$ increased with calcination temperature without the appearance of impurity phases. The series of oxide precursors calcined at above 773 K and below 1023 K for 12 h were amorphous. The surface area measured by N$_2$ adsorption at 77 K was 60 m^2 g^{-1} for the amorphous precursor prepared at 773 K. The surface area decreased with increasing calcination temperature, such that the crystalline Sm$_2$Ti$_2$O$_7$ prepared at 1473 K had a surface area of only 0.36 m^2 g^{-1}.

Sulfurization of Oxide Precursor. Figure 3 shows the XRD patterns of various oxide precursors after
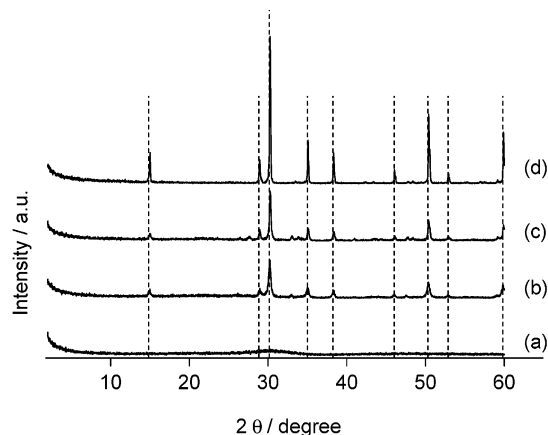

Figure 2. XRD patterns of oxide precursors prepared at (a) 773 K for 12 h, (b) 1073 K for 5 h, (c) 1273 K for 5 h, and (d) 1473 K for 5 h.
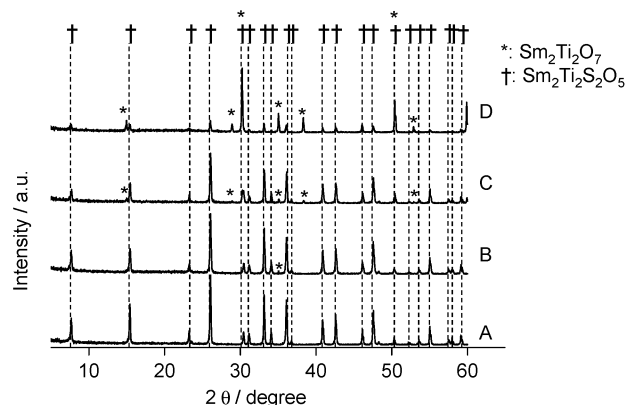

Figure 3. XRD patterns of oxide precursors sulfurized under H$_2$S flow at 1273 K for 5 h. Precursors were prepared by calcination at (A) 773 K for 12 h, (B) 1073 K for 5 h, (C) 1273 K for 5 h, and (D) 1473 K for 5 h.

sulfurization at 1273 K for 5 h. The sulfurized samples A, B, C, and D correspond to the oxide precursors a, b, c, and d in Figure 2. Sample A included a single phase of Sm$_2$Ti$_2$S$_2$O$_5$, whereas samples B, C, and D exhibited two distinct phases of Sm$_2$Ti$_2$S$_2$O$_5$ and Sm$_2$Ti$_2$O$_7$. Sample A, calcined at 773 K, exhibits only a single phase of Sm$_2$Ti$_2$S$_2$O$_5$ upon sulfurization, and is therefore the most suitable sample for sulfurization and synthesis of Sm$_2$Ti$_2$S$_2$O$_5$. In all samples prepared hereafter, the oxide precursor was calcined at 773 K.

Figure 4 shows the XRD patterns of Sm$_2$Ti$_2$S$_2$O$_5$ obtained at various temperatures by the proposed method. Diffraction peaks corresponding to Sm$_2$Ti$_2$S$_2$O$_5$ appeared for the sample sulfurized at 1073 K even after 1 h. After 10 h sulfurization at 1073 K, the diffraction peaks of Sm$_2$Ti$_2$O$_7$ disappeared. At sulfurization temperature of 1123 K or above, a single phase of Sm$_2$Ti$_2$S$_2$O$_5$ was obtained even after a short period of sulfurization (1 h). Thus, the proposed method allows for very quick synthesis of Sm$_2$Ti$_2$S$_2$O$_5$ compared to the solid-state method, which took up to 2 weeks. Figure 5 shows the variation in crystallite size of Sm$_2$Ti$_2$S$_2$O$_5$ with sulfurization temperature. Each sample was sulfurized for 1 h at the stated temperature. The crystallite sizes of Sm$_2$Ti$_2$S$_2$O$_5$ powders were determined by the Scherrer equation, using the (013) reflection of Sm$_2$Ti$_2$S$_2$O$_5$ for calculation. The crystallite size of
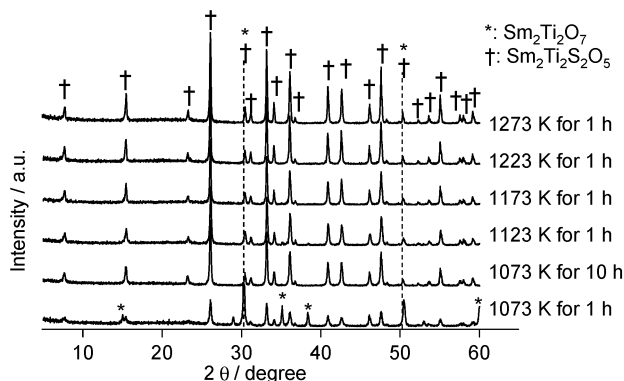
Figure 4. XRD patterns of $Sm_2Ti_2S_2O_5$ (HGS) obtained at various temperatures
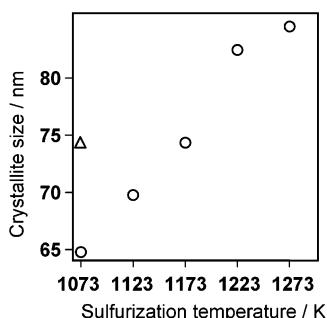
**Figure 5.** Variation in crystallite size of $Sm_2Ti_2S_2O_5$ with sulfurization temperature. Open triangle: after 10 h sulfurization. Open square: after 1 h sulfurization.
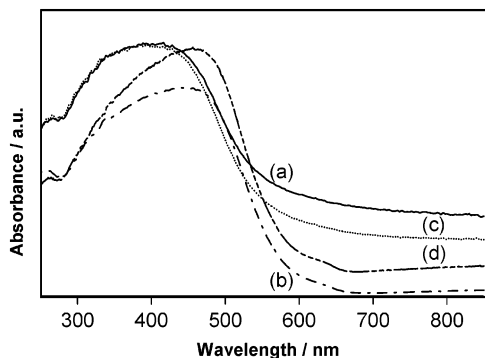

Figure 6. UV−vis DRS spectra of (a) $Sm_2Ti_2S_2O_5$ (HGS, 1173 K for 1 h), and (b) $Sm_2Ti_2S_2O_5$ (SSR), and after heating sample (a) in air at 473 K for 2 h (c), and in a sealed quartz tube with S at 1273 K for 4 days (d).

$Sm_2Ti_2S_2O_5$ increased gradually with sulfurization temperature from 1073 to 1123 K. The crystallite size of $Sm_2Ti_2S_2O_5$ prepared at 1073 K for 1 h was estimated to be ca. 65 nm, and continued to grow with sulfurization time.

Characterization of $Sm_2Ti_2S_2O_5$. The UV−vis DRS spectra of $Sm_2Ti_2S_2O_5$ (HGS, 1173 K, 1 h) and $Sm_2Ti_2S_2O_5$ (SSR) are shown in Figure 6. The absorption edge at 600 nm was observed for both samples, whereas an absorption in the near-infrared region beyond 600 nm was also observed only for $Sm_2Ti_2S_2O_5$ (HGS). This near-infrared absorption is attributed to the existence of a small amount of Ti^{3+} species in the sample, reduced from Ti^{4+} by exposure of the oxide precursor to H_2S. The spectra of $Sm_2Ti_2S_2O_5$ (HGS) after heat treatment in air at 473 K for 2 h and in a vacuum at 1273 K for 4 d are shown in Figures 6(c) and (d). Heat
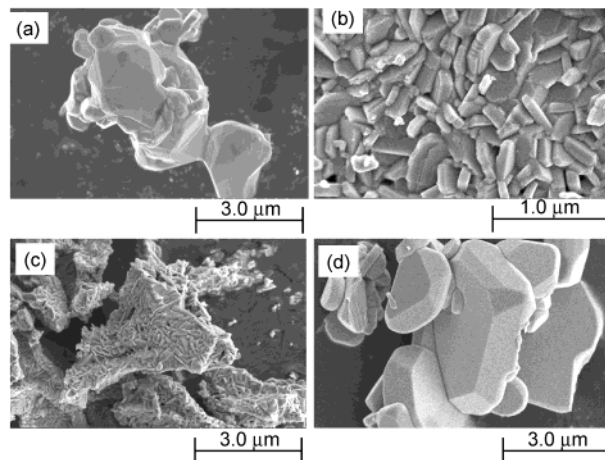

Figure 7. SEM images of $Sm_2Ti_2S_2O_5$ produced by (a) the SSR method, (b and c) the HGS method, and (d) the HGS method followed by heating in a vacuum at 1273 K for 4 days.
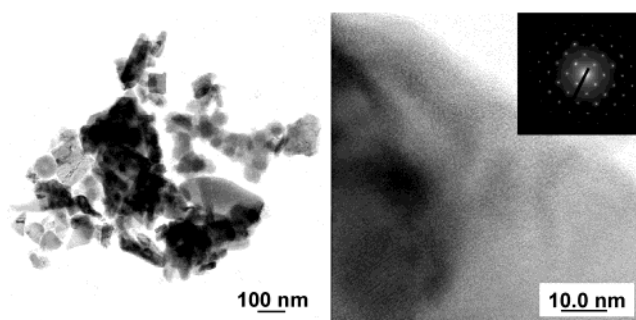
Figure 8. TEM image and electron diffraction pattern of $Sm_2Ti_2S_2O_5$ (HGS, 1173 K).

treatment in a vacuum was carried out by calcining a mixture of $Sm_2Ti_2S_2O_5$ (HGS, 1.0 g) and sulfur (0.2 g) in a sealed quartz tube. Heating the $Sm_2Ti_2S_2O_5$ (HGS) in air or vacuum resulted in a weakening of the absorption band above 600 nm. Heat treatment did not change the crystal structure or bulk composition, but appeared to cause Ti^{3+} to oxidize to Ti^{4+}, as indicated by XRD and energy-dispersive X-ray spectroscopy (EDX).

Figure 7 shows SEM images of $Sm_2Ti_2S_2O_5$ prepared by the SSR and HGS methods. In the case of $Sm_2Ti_2S_2O_5$ (SSR), round particles (2−4 μm) were observed, and the surface area as measured by N_2 adsorption at 77 K was 0.6 m^2 g^{-1}. In the case of $Sm_2Ti_2S_2O_5$ (HGS), platelike particles with smooth surfaces were obtained. This morphology was relatively constant, and independent of sulfurization temperature. SEM observation of $Sm_2Ti_2S_2O_5$ (HGS) revealed that primary particles of about 0.1−0.5 μm diameter aggregate to form large secondary particles of 0.5−5.0 μm. The difference in the particle size between those calculated by the Scherrer's equation and those observed by SEM suggests that the particles observed by SEM are the polycrystalline particles. The surface area of the $Sm_2Ti_2S_2O_5$ (HGS) sample was 6 m^2 g^{-1}. Therefore, the HGS method provides a 10-fold increase in surface area compared to that of the SSR method. An SEM image of $Sm_2Ti_2S_2O_5$ after heating in a vacuum at 1273 K for 4 days is shown in Figure 7(d). Heating resulted in an increase in $Sm_2Ti_2S_2O_5$ particle size, and the morphology became essentially the same as that of the $Sm_2Ti_2S_2O_5$ (SSR) sample. A TEM image of $Sm_2Ti_2S_2O_5$
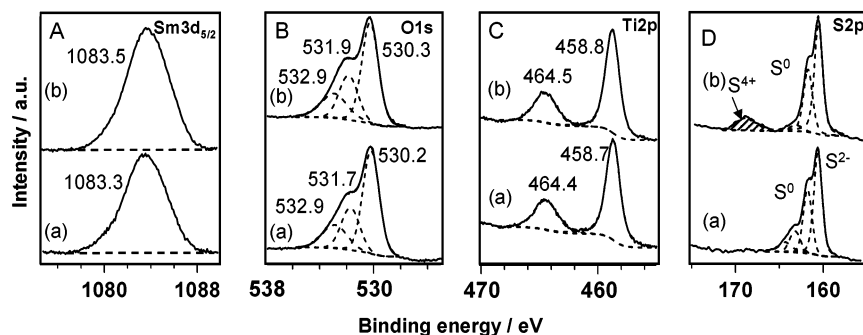
Figure 9. XPS spectra for (A) Sm3d$_{5/2}$, (B) O1s, (C) Ti2p, and (D) S2p of Sm$_2$Ti$_2$S$_2$O$_5$ before and after heat treatment in air at 473 K for 2 h.

Table 1. Surface Atomic Ratios of Sm/Ti, S/Ti, and O/Ti of Sm$_2$Ti$_2$S$_2$O$_5$ Before and After Heat Treatment

		S/Ti			
sample	Sm/Ti	S^{2-} (160.8 + 162.0 eV)	S^0 (163.3 + 164.8 eV)	S^{4+} (168.2 + 169.4 eV)	O/Ti
before HT	0.9	1.2	0.2	0.0	3.0
after HT	0.9	1.2	0.1	0.2	3.0

(HGS) prepared at 1173 K for 1 h is shown in Figure 8. The TEM image and electron diffraction pattern indicate that well-crystallized Sm$_2$Ti$_2$S$_2$O$_5$ is formed by sulfurizing for 1 h. The particle size calculated by the Scherrer's equation is almost coincident with that observed by TEM.

Figure 9 shows the XPS spectra of Sm$_2$Ti$_2$S$_2$O$_5$ (HGS) before and after heat treatment in air at 473 K for 2 h. The surface atomic ratios of Sm/Ti, O/Ti, and S/Ti are summarized in Table 1. The surface atomic ratio of O/Ti was estimated from the O1s peak at 530 eV.[6] Two S species were observed for Sm$_2$Ti$_2$S$_2$O$_5$ before heat treatment (Figure 9D(a); one assigned to S^{2-} species (S2p3/2, 160.8; 2p1/2, 162.0 eV) and the other to S^0 (S2p3/2, 163.3 eV; 2p1/2, 164.8 eV) deposited on the surface of Sm$_2$Ti$_2$S$_2$O$_5$. The features of the XPS spectra remained unchanged after heat treatment except for the S2p peaks. The surface atomic ratios of Sm/Ti, O/Ti, and S/Ti (S^{2-}) also remained unchanged. After heat treatment, the intensity of the S^0 peaks (163.3 and 164.8 eV) decreased and new peaks appeared at 168.2 (S2p3/2) and 169.4 eV (2p1/2), assigned to S^{4+} species (Figure 9D(b)). This indicates that the adsorbed sulfur S^0 species was oxidized by heat treatment. The S^{4+} species disappeared after the sample was suspended in water (data not shown). It is therefore considered that sulfur species other than S^{2-} can be removed by heat treatment. The XPS results indicate that heat treatment in air oxidizes S^0 species on the surface of Sm$_2$Ti$_2$S$_2$O$_5$ to S^{4+}, whereas the surface S^{2-} species of Sm$_2$Ti$_2$S$_2$O$_5$ remain essentially unchanged.

Photocatalytic Activity of Sm$_2$Ti$_2$S$_2$O$_5$. Table 2 shows the dependence of the photocatalytic activity of Sm$_2$Ti$_2$S$_2$O$_5$ (HGS) upon sulfurization temperature. O$_2$ evolution was examined in a basic solution (ca. pH 8) buffered by La$_2$O$_3$.[8,9] The pH of the aqueous Na$_2$S−Na$_2$SO$_3$ solution for H$_2$ evolution was 13. Pt as an H$_2$ evolution promoter was loaded by impregnation from H$_2$PtCl$_6$, followed by reduction in H$_2$ at 473 K. The

(9) Kasahara, A.; Nukumizu, K.; Hitoki, G.; Takata, T.; Kondo, J. N.; Hara, M.; Kobayashi, H.; Domen, K. *J. Phys. Chem. A* **2002**, *106*, 6750.

Table 2. Dependence of Photocatalytic Activity of Sm$_2$Ti$_2$S$_2$O$_5$ on Calcination Temperature

	rate of gas evolution (μmol/h)			
	O$_2$		H$_2$	
sulfurization temp (K)^a	before HT	after HT (473 K, 2 h)	before HT	after HT (473 K, 2 h)
1073^b	6	10	0.3	6
1123	15	17	6.6	22
1173	12	20 [10]^c	0.9	22 [8]^c
1223	9	12	0.2	8
1273	5	8	1.5	5

^{a} Sulfurization for 1 h. ^{b} Sulfurization for 10 h. ^{c} After heat treatment at 1273 K for 4 d in a vacuum.

highest activity of H$_2$ or O$_2$ evolution was obtained for the sample prepared at 1123 K for 1 h. The photocatalytic activity of Sm$_2$Ti$_2$S$_2$O$_5$ prepared at 1073 K for 10 h was lower than that of the sample prepared at 1123 K for 1 h due to lower crystallinity. The photocatalytic activity decreased with increasing sulfurization temperature from 1123 to 1273 K due to particle growth and the generation of Ti^{3+} species. The steady-state quantum efficiency for H$_2$ evolution was 0.07%, and that for O$_2$ evolution was estimated to be 0.4% for the Sm$_2$Ti$_2$S$_2$O$_5$ sample prepared at 1123 K for 1 h. In contrast, the quantum efficiencies of H$_2$ and O$_2$ evolutions for Sm$_2$Ti$_2$S$_2$O$_5$ (SSR) were estimated to be 0.3% and 0.2%, respectively. The proposed synthesis route therefore provides catalysts with enhanced photocatalytic activity for O$_2$ evolution, yet with decreased activity for H$_2$ evolution. The low activity for H$_2$ evolution is expected to be due to the presence of Ti^{3+} species in the bulk and S^0 species on the Sm$_2$Ti$_2$S$_2$O$_5$ surface. The presence of Ti^{3+} species in the sample means the existence of the vacancies. The vacancies would work as recombination centers for photoexcited electrons and holes to reduce the efficiency. It is also considered that S^0 species interfere with the deposition of Pt on Sm$_2$Ti$_2$S$_2$O$_5$ surface. Pt was indispensable for H$_2$ evolution reaction. In the case of O$_2$ evolution reaction, no cocatalyst is needed for Sm$_2$Ti$_2$S$_2$O$_5$ and S^0 species is oxidized during O$_2$ evolution reaction. Therefore, the activity for O$_2$ evolution was little affected by the presence of S^0 species. Table 2 also shows the photocatalytic activities of Sm$_2$Ti$_2$S$_2$O$_5$ (HGS) after heat treatment in air or a vacuum. Heating in air at 473 K for 2 h enhanced photocatalytic activities for both H$_2$ and O$_2$ evolution. After this heat treatment, the Sm$_2$Ti$_2$S$_2$O$_5$ sample prepared at 1173 K for 1 h exhibited a quantum efficiency for H$_2$ and O$_2$ evolution of 0.3% and 0.6%, respectively. It is considered that the decrease

of S^0 species on the surface and the vacancies in the bulk by heating in air brought about the enhancement of the photocatalytic activities. The H_2 evolution activity (22 μmol/h) of $Sm_2Ti_2S_2O_5$ (HGS) was equivalent to that (18 μmol/h) of $Sm_2Ti_2S_2O_5$ (SSR) because the removal of the vacancies and S^0 species was not complete, as shown in Figures 6 and 9. Heating $Sm_2Ti_2S_2O_5$ in a vacuum at 1273 K for 4 d with sulfur resulted in a decrease in the photocatalytic activities. Although the concentration of Ti^{3+} species in the bulk decreased by heat treatment in a vacuum, the abundance of S^0 species on the surface increased and the surface area decreased. This increased prevalence of S^0 species on the surface and the lower surface area are considered to be responsible for the reduced photocatalytic activities.

The proposed method can produce $Sm_2Ti_2S_2O_5$ with equivalent H_2 and superior O_2 evolution activity compared to that of the solid-state method, with a far shorter preparation time and at lower temperature. It is expected that the complete removal of the vacancies and S^0 species enhance photocatalytic activities.

Conclusion

A new method for the synthesis of oxysulfide $Sm_2Ti_2S_2O_5$ using H_2S was presented. The photocatalytic activities of the catalyst produced by this method were improved by heating in air at 473 K for 2 h. This new method allows $Sm_2Ti_2S_2O_5$ to be synthesized with a much shorter heating period (1 h) and at much lower temperature than those used for the previous solid-state method. Synthesis under H_2S flow is expected to be applicable to the preparation of other oxysulfide catalysts with high activities and is currently under investigation.

CM034540H